This paper was presented to the 3rd Emission Solutions in Transportation,
AFS International Conference, Oct. 25 - 27, 2007, Ann Arbor, Michigan, U.S.A.

Infrared-Excitation for Improved Hydrocarbon Fuel's Combustion Efficiency

Albert C. Wey
Aldi Far-Infrared Products, Inc.

Rodney G. Handy
Dept. of Mechanical Engineering Technology
Purdue University

Yuan Zheng and Chul H. Kim
Maurice J. Zucrow Laboratories
Purdue University

Copyright © 2007 AFSS

ABSTRACT

Photoexciting hydrocarbons with infrared shorter than 20 microns in wavelengths for enhanced fuel conversion efficiency are believed to be scientifically predictable. This paper describes a scientific investigation in the concept using infrared excitation for increased hydrocarbon fuels' combustion efficiency. The IR-effect on flame structure is studied in a widely-used counterflow methane-air diffusion flame experiment. Species concentrations for H_2, O_2, N_2, CH_4, CO, CO_2, C_2H_2, and C_2H_4 across the flame were measured using sampling and gas chromatography while NO (nitric oxide) concentrations were measured using chemiluminescence analysis. The experimental results indicate IR-excitation makes fuel more combustible and burn faster than regular fuel. As a result of faster combustion, the fuel consumption rate and peak CO and NO emissions are reduced. IR-excitation was applied in several engine and vehicle tests to examine its effects on improving engine efficiency. The results suggest IR-excitation can significantly improve engine performance for increased fuel economy and reduced emissions.

INTRODUCTION

Using infrared-excited fuels for improved fuel efficiency of internal combustion engines was first disclosed in 2003 [1]. Hydrocarbons are IR-active and absorb multi-photons in 3 – 14 μm wavelengths, causing molecular vibrations [2]. Photochemistry enhancement of reaction rates by reactant vibrational excitation have been demonstrated in laboratory dynamics studies [3]. These scientific facts suggest that by IR-exciting hydrocarbon fuels combustion efficiencies will be significantly enhanced. Though photoexciting hydrocarbon molecules for enhanced fuel conversion efficiency are believed to be scientifically predictable, a broadband IR-excitation source that could facilitate the proposed applications did not commercially exist. Adopting the IR technology that prevailed in Japan, we engineered an IR-ceramic from selective transition metal oxides that emit 3 - 14 μm wavelength mid-infrared [4]. In engine applications, the IR-emitting ceramic can be clamped to the exterior of a nonmetal supply fuel line, since 3 – 14 μm wavelength photons can penetrate nonmetal materials. Hydrocarbons traversing thorough the fuel line are exposed to infrared radiation and excited before the fuel enters cylinders for combustion. Confirmatory test results demonstrating IR-effect on improving engine performance to significantly improve fuel economy and emissions were reported [5]. In that report, all targeted emissions from engines, including THC, CO, and NOx, were simultaneously reduced. Nevertheless, how IR-excitation participates in the thermochemical process of combustion to improve fuel's conversion efficiency remains unidentified.

The combustion of multi-component commercial fuels (e.g. gasoline, diesels) in an engine involves many complicated processes, such as atomization, evaporation, turbulent mixing, and combustion timing. To eliminate the complexities in a gasoline or diesel engine, laminar non-premixed counterflow methane-air flame experimentation was used at Zucrow Laboratories, Purdue University to investigate the IR-effect on combustion of methane, the simplest form of hydrocarbon fuel, in the present study. Counterflow flames are widely used in evaluation of chemical kinetic rates because they are one-dimensional and have a uniform strain rate [6]. Counterflow flames also allow the use of OPPDIF code developed by Sandia [7,8] to reveal chemical kinetics details with manageable computational times. Besides, the methane mechanism and the thermochemical database given in GRI-Mech 2.11 [9] can be used to predict and compare the measured concentrations of major species in the flame.

The present study has successfully demonstrated the IR-excitation effect on influencing methane flame structure (i.e. distribution of species across the flame) with reduced pollutant (CO, and NO) emissions. Preliminary results are very encouraging, indicating the IR-effect is existent. The IR-effect was verified on a single-cylinder engine to reduce CO and NOx and on a Ford F-350 diesel truck to simultaneously reduce fuel consumption and emissions. In this paper the hypothetical model is described and results are presented.

ABSORPTION OF INFRARED RADIATION

When a photon is absorbed by a molecule, it ceases to exist and its energy is transferred to the molecule. This energy can be transferred to vibrational, rotational, electronic, or translational forms. Excitation of vibrational modes in a molecule requires a photon with wavelength typically shorter than 20 μm. Examination of the geometry of the molecule can tell if a molecule will be infrared-active. Hydrocarbons are IR-active and absorb IR photons to cause molecular vibrations. Some exemplary IR-excited vibrations in hydrocarbons are listed in Table 1.

Table 1. IR absorptions by hydrocarbon molecules.

ω (cm^{-1})	λ (μm)	Bond Structure
1315 – 1475	6.78 – 7.60	C–H (in *alkanes*)
2800 – 3000	3.33 – 3.57	C–H (in *alkanes*)
1450 – 1600	6.25 – 6.90	C=C bond in *aromatic ring*
1650 – 1670	5.99 – 6.06	C=C
2100 – 2260	4.42 – 4.76	C≡C
3000 – 3100	3.23 – 3.33	C–H (part of *aromatic ring*)
3300	3.03	C–H (C is *acetylenic*)
3020 – 3080	3.25 – 3.31	C–H (C is *ethylenic*)
1420–1470	6.80–7.04	Alkanes' $-CH_3$
1375	7.27	Alkanes' $-CH_3$
1430–1470	6.80–6.99	Alkanes' $=C H_2$
1370, 1385	7.30, 7.22	Alkanes' $-CH(CH_3)_2$
1170	8.55	Alkanes' $-CH(CH_3)_2$
1370, 1395	7.30, 7.17	Alkanes' $-C(CH_3)_3$
910–920	10.87–10.99	*Alkenes' $RCH=CH_2$
990–1000	10.00–10.10	*Alkenes' $RCH=CH_2$
880 – 900	11.11–11.36	*Alkenes' $R_2C=CH_2$
675 – 730	13.70–14.81	*Alkenes' RCH=CHR *cis*
965 – 975	10.26–10.36	*Alkenes' RCH=CHR *trans*
730 – 770	12.99–13.70	*Aromatic C–H (1)
735 – 770	12.99–13.61	*Aromatic C–H (2) *ortho*
690 – 710	14.08–14.49	*Aromatic C–H (2) *meta*
750 – 810	12.35–13.33	*Aromatic C–H (2) *meta*
810 – 840	12.35–11.90	*Aromatic C–H (2) *para*

* means "Out-of-Plane"; (1) Mono-substituted; (2) Distributed.

For example, the C≡C bond in hydrocarbon molecule has a higher force constant than C=C bond so that C≡C bond absorbs IR at a higher frequencies (i.e. higher energy) at 2100 – 2260 cm^{-1} (or 4.76 – 4.42 μm wavelengths) than the C=C bond at 1650 – 1670 cm^{-1} (6.06 – 5.99 μm). It takes more energy to make the stronger C≡C bond vibrate than it does to the C=C bond. Organic chemists have been using the IR absorption spectral information (called Infrared Correlation Charts) to identify hydrocarbon specimens for many decades [10].

MOLECULAR VIBRATIONS

Photoselective Chemistry is concerned with the influence of selective optical excitation on the acquisition, storage and disposal of energy and on the reactivity of molecules. Classic work of Evans and Polanyi in the 1930s illustrated the importance of molecular vibrational energy in reaction dynamics [11]. It was recognized early in the study of chemical kinetics that increasing the energy of reactants increased reaction rate, which was usually accomplished by simply raising the reaction temperature. However, Evans and Polanyi presented the argument that the reactant vibrational energy is the most effective at promoting reaction. As experimental techniques were refined, it became possible to demonstrate that increasing vibrational energy is indeed relatively more important than raising temperature in enhancing a molecular reaction. The expectation is that if vibrational excitation is sufficient to raise the system and lower the activation barrier, substantial rate enhancement would be realized.

Tunable lasers provide a very convenient method for obtaining selective vibrational excitation. A number of reactions of IR laser-excited species have been studied. The correlation between ground-state heats of reaction and vibrationally induced reaction rate enhancement is striking for these processes. Vibrational energy in some of these cases was found to enhance the reaction rate by two orders of magnitude [12]. It is concluded that chemical reactions can be drastically enhanced by optical excitation from infrared lasers.

INFRARED MULTIPHOTON ABSORPTION AND EXCITATION

The discovery that polyatomic molecules under collision-free conditions may absorb many infrared quanta from an IR laser had generated interests regarding molecular multiphoton process (MMP). Based on the currently available experimental information and theoretical studies, a qualitative picture can be drawn as in Fig.1 [13]:

The molecular energy levels can be separated into three regions [14]. In the lowest energy range (region I) the density of molecular states is very low and the IR field is interacting with isolated molecular states. In this region, multi-photon resonances are accounted for in terms of the molecular level-scheme of region I.

After the molecule absorbs a few quanta, the density of molecular states becomes very large, and we can no longer describe the time evolution in terms of few isolated molecular states. This region is denoted region II, quasi-continuum, involving intramolecular energy transfer and line broadening (dephasing).

Finally, when the molecule has acquired enough energy for dissociation, it enters the region III, where we have to incorporate the dynamics of unimolecular decomposition.

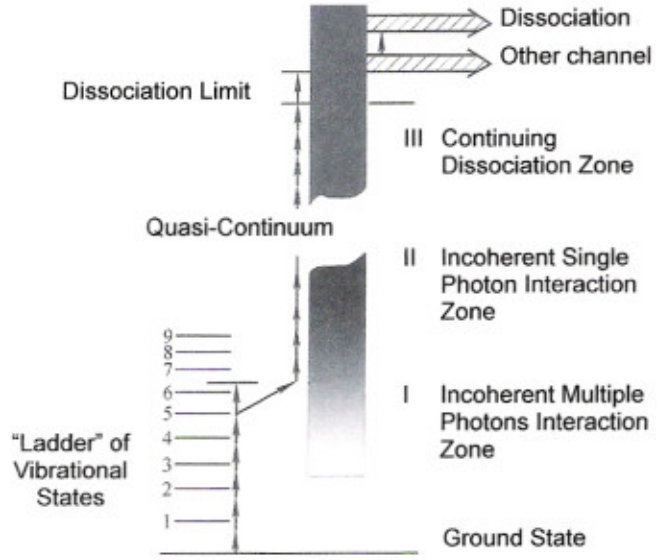

Fig. 1 Molecular level scheme for Infrared Multiphoton Excitation and Dissociation.

METHANE VIBRATIONAL ENERGY LEVELS

To illustrate the complexity of the molecular vibrations caused by IR-excitation, we can use the energy-transfer in methane (CH_4) as an example.

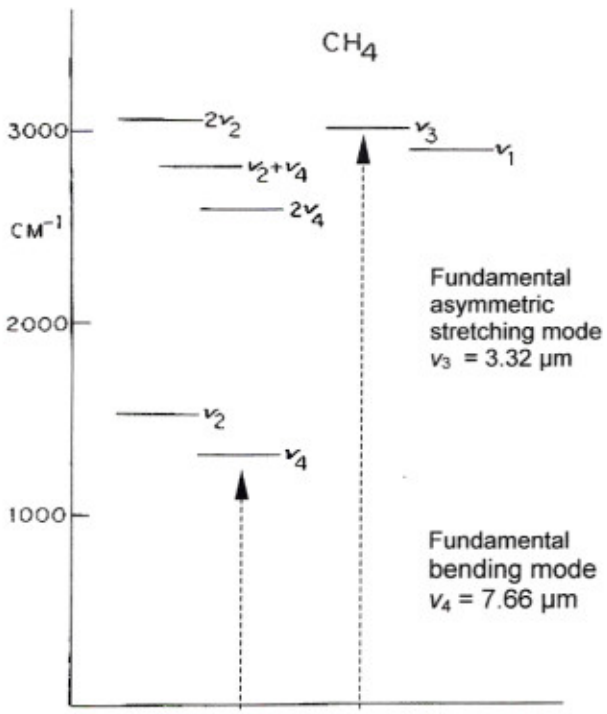

Fig. 2 Partial vibrational energy level diagram of CH_4.

Methane (CH_4) was the first polyatomic molecule for which vibrational energy-transfer pathways and rates were investigated [15]. Single Modes, or fundamental vibration energy levels of methane include asymmetric stretching vibration v_3 at 3010 cm^{-1} (3.32 μm), bending mode v_4 at 1306 cm^{-1} (7.66 μm), and v_1 and v_2, which are the equilibration of v_3 and v_4, respectively. Methane's vibrational energy levels may also include combination modes and overtones such as $2v_4$, $v_2 + v_4$, and $2v_2$. Further equilibration of states is postulated to occur involving more overtones and combination bands, though fully comprehending the system is impossible.

According to Figures 1 and 2, methane molecules absorb a number of IR photons that match its fundamental and/or combination modes to climb up the ladder of vibrational states. As such, IR-excited methane molecules are in excited states where the activation barrier of reaction is lowered as shown in Fig. 3. The activation barrier is the potential energy of reactants required to be overcome in order for the reaction to take place [16]. The height of the activation barrier (or the activation energy required) between reactants and products determines the rate at which the reaction may occur. The lower the activation barrier is, the better the reaction rate will be, as it will take less energy to break up an excited methane molecular structure.

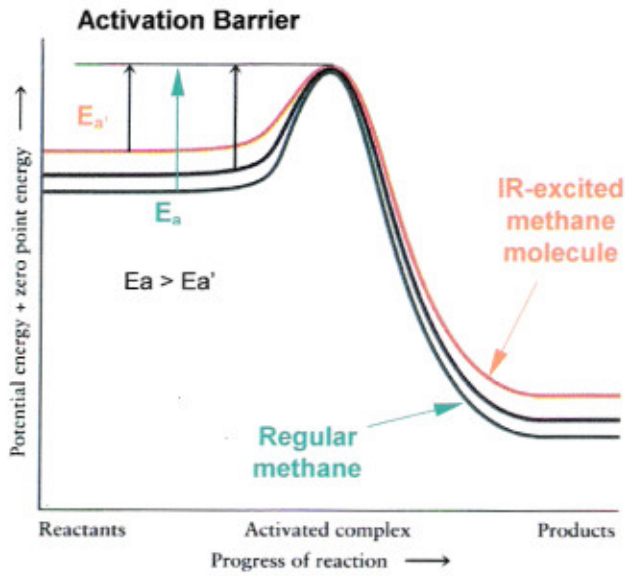

Fig. 3 Reaction profiles of regular and IR-excited methane.

The reaction rate W is determined by Arrhenius equation:

$$W = k\, e^{-E/RT}$$

Where k is a constant, R the universal gas constant, T temperature in °K, E the activation energy (the energy required to overcome activation barrier). The lower the activation barrier is, the higher the reaction rate will be. As previously stated, in early study of chemical kinetics increasing reaction rate was usually accomplished by raising the reaction temperature T. However, Evans and Polanyi suggested that the increasing reactant vibrational energy (i.e. reducing required activation energy E) is the

most effective at promoting reaction. In experiments, increasing reactants vibrational energy was indeed found to enhance the reaction rate more significantly than simply raising the reaction temperature.

FABRICATION OF IR-EMITRERS

Broadband IR-emitters comprised of metal oxides have been broadly used in Japan for agricultural applications since the 1960's. Japanese are particularly successful in using 8 – 20 μm "far-infrared" (but categorized as "mid-infrared" by NASA) in heating and drying agricultural produces for preserve. Prolific experimental data that characterize IR-emitting metal oxides are available in Japan. Based on this known Japanese research, we could tailor IR-emitters using selective transition metal oxides to emit 3 - 14 μm wavelengths.

Transition metal oxide has such a unique property that its constituent electrons can be thermally agitated to reach a neighboring higher energy level; when the excited electron returns to its initial level, it emits IR photons in 3 - 14 μm wavelength range, depending on the variety of oxides used. We had made a 3 - 14 μm IR-emitter for our fuel applications by adding ZrO_2, CoO, and other oxides to $2MgO{\cdot}2Al_2O_3{\cdot}5SiO_2$, one of the most popular IR ceramics in Japan [5]. An IR-emitting composite can be made by sintering the mixture of selected oxides powders and bonding agents at above 1300 °C. The resultant ceramic composite continuously absorb ambient heat and emit IR photons in 3 - 14 μm wavelengths. Thus, IR emissions can last indefinitely. In essence, the IR-ceramic is an energy converter that absorbs ambient heat and converts it into IR photons to maintain thermal equilibrium.

An SEM/EDS (scanning electron microscope with energy dispersive spectrometry) plot was run with IR-emitter to obtain a quantitative analysis showing general elemental composition of the oxide compounds. The results are presented in Table 2.

Table 2. Elemental composition of the oxide compounds.

Element	Wt.%	Cmpt.	CmptWt%	Cnts/s	Atomic %
O*	41.12				60.41
Na	0.70	Na_2O	1.18	5.85	0.71
Mg	5.58	MgO	9.25	70.52	5.40
Al	14.19	Al_2O_3	26.80	208.33	12.36
Si	17.73	SiO_2	37.93	261.02	14.84
K	1.35	K_2O	1.62	17.41	0.81
Fe	1.04	Fe_2O_3	1.48	6.69	0.44
Co	1.43	CoO	1.82	7.77	0.57
Zn	1.18	ZnO	1.47	3.67	0.43
Zr	15.69	ZrO	18.44	0.93	4.04

Sample conditions: 20.0 KV; Beam Current (175.0 picoAmps); Tilt Angle (0 deg.); Working Distance (20 mm); TakeOff Angle (35.6°); Solid Angle*BeamCurrent: 1.4.

For the ease of implementation, a partial-tubular shape is designed as shown in Fig. 4, which can easily be tied to the exterior of a non-metal fuel supply line of engines to absorb engine radiation heat and emit infrared.

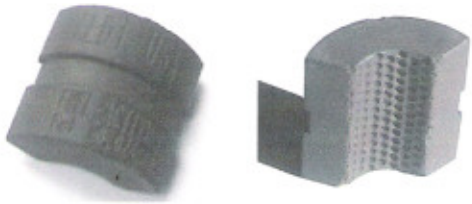

IR-emitter Top View Bottom View

Fig. 4 Picture of IR-emitter, 1" x 1" x 3/8" in size.

METHANE-AIR COUNTERFLOW EXPERIMENTS

Counterflow flames are widely used in the evaluation of chemical kinetic rates because they are one-dimensional and have a uniform strain rate. The experiments were performed at Purdue's Zucrow Laboratories and the geometry of the burner is similar to the one designed by Puri et al [17] as shown in Fig. 5, with a picture of laminar flame in Fig. 6.

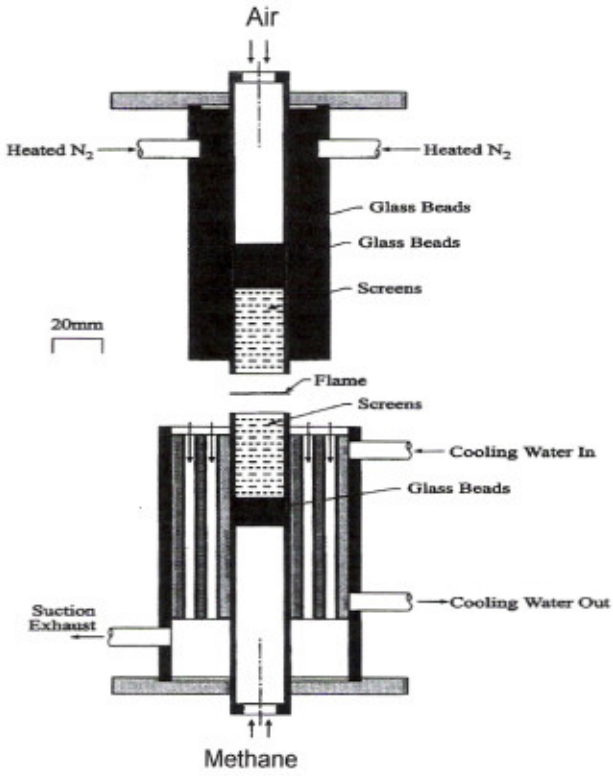

Fig. 5 Schematic of the counterflow burner.

Fig. 6 Opposed-flow flame, flow speed = 25 cm/s.

Numerical Predictions

A detailed description of equations governing conterflow flames is given by Kee et al. [8]. The OPPDIF code was used to predict the flame structure. The energy equation in the code involves variable specific heat, variable thermal conductivity, and variable mass diffusion velocities for the different species and a volumetric energy source term involving all reaction steps. All thermophycal properties were taken from the GRI-Mech 2.11 thermo-dynamic database [9]. Fig. 7 shows an exemplar of numerical predictions of mole fractions for various species (CH_4, N_2, CO, CO_2 and NO) across the counterflow flame, plotted as a function of distance from the fuel duct, in which the flame locates at where the fuel (CH_4) mole fraction reach its minimum value.

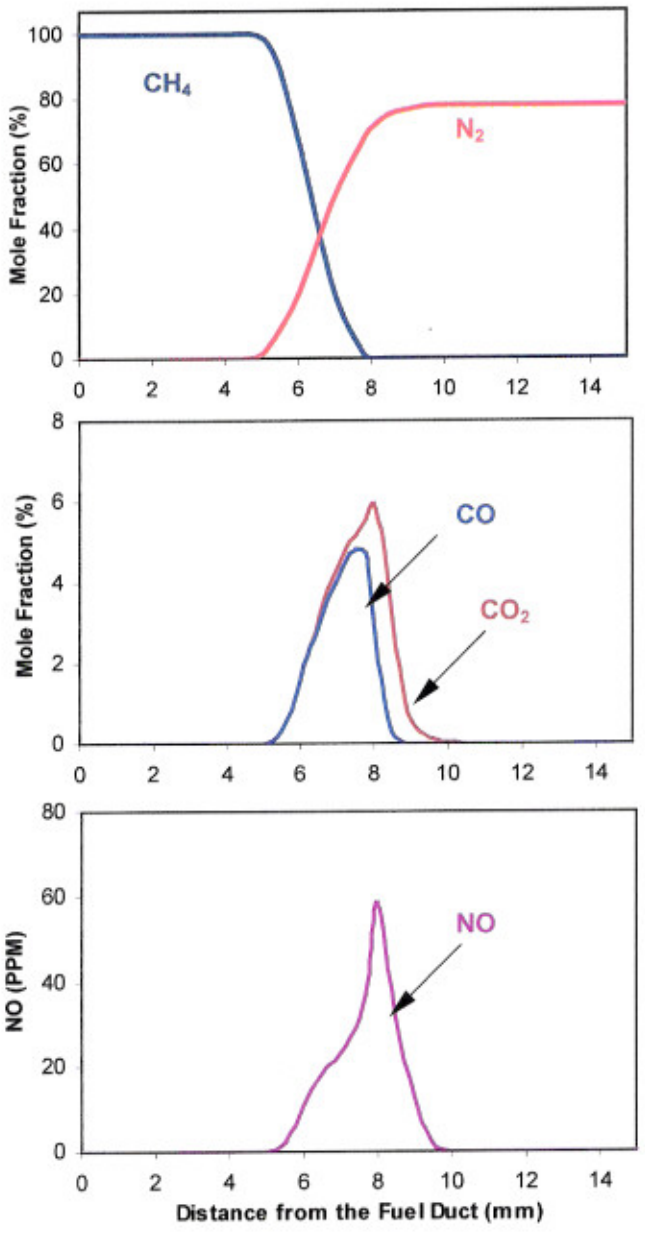

Fig. 7 Numerical predictions of species CH_4, N_2, CO, CO_2, and NO mole fractions across the flame at a flow speed = 25 cm/s.

RESULTS AND DISCUSSION

The experiments were performed with methane (Airco Gas and Gear, 99% methane) introduced from the bottom duct and air from the top duct. A nitrogen coflow was introduced from the top duct to stabilize the flames. The separation distance between the two ducts is 15 mm and the inner diameter of both ducts is 20 mm. The velocity is 10 cm/sec, calculated assuming uniform flow at the exit. In order to verify the effect of infrared excitation on the fuel, a control valve, as shown in Fig. 8, was used to selectively direct the fuel through either a regular Teflon line (for Baseline measurements) or the line with IR-emitters attached to it (for IR-excited measurements).

Measurements of mole fraction of gas species were made using a quartz microprobe, which had an outer diameter of 2.97 mm and a conical tip reducing the frontal outer diameter to 0.5 mm over a distance of 10 mm. The inner diameter was 0.080 mm. Gas samples along the line of symmetry were withdrawn at various axial distances from the fuel tube by positioning the probe at a radial distance of 1 mm near the axis. Species distributions in the flame were measured by using a gas chromatograph (GC) (Shimadzu, GC8A). The nitric oxide (NO) distribution was measured using a calibrated chemiluminescence analyzer (Thermo Environmental Instruments, 42H).

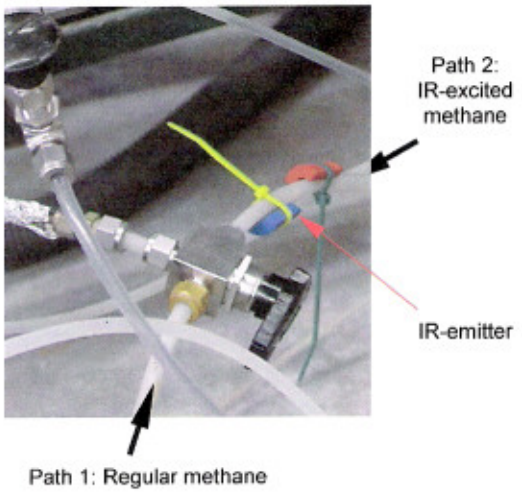

Fig. 8 Controllable feeding paths for methane.

Measured N_2 and CH_4 Distributions

Fig. 9 shows measured mole fractions of N_2 and CH_4, plotted as a function of distance from an approximate center between the fuel duct and the air duct, both ducts being separated at a distance of 15 mm. The data show that the flame location where the fuel CH_4 mole fraction reaches its minimum value moves toward the fuel duct because the momentum of the fuel stream decreases with IR-excitation at a constant velocity. The plotted curves of measured N_2 and CH_4 mole fractions of IR-excited fuel moving toward the fuel duct indicates that diffusion flame occurs earlier, meaning IR-excited fuel combusts faster than regular fuel.

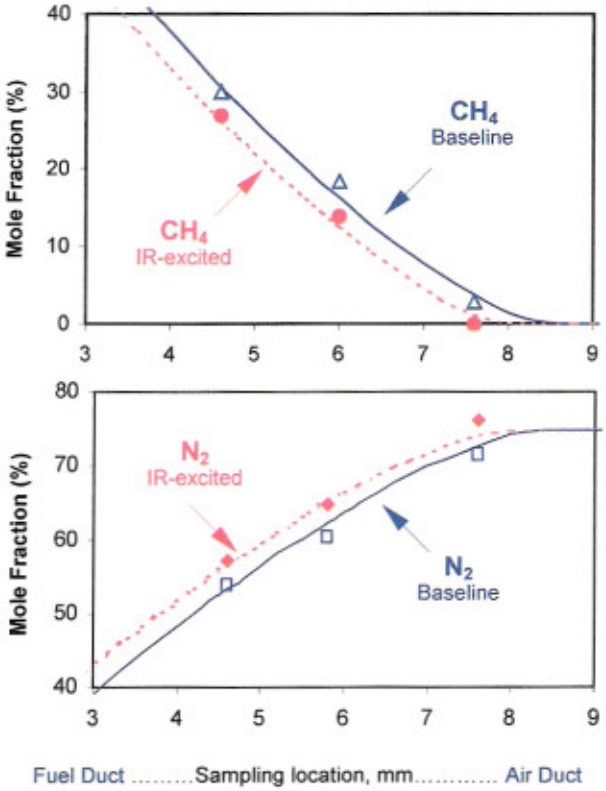

Fig. 9 Measurements of N_2 and CH_4 mole fractions.

The lines associated with measured data points shown in Fig. 9 are computational predictions made by using OPPDIF code.

Meanwhile, the fuel consumption rate can be calculated by integrating the net volumetric consumption rate over the entire computational domain [18]:

$$Fuel\ Consumption\ Rate = \int_0^L \varpi_{CH4}\, dx$$

where L is the distance between the ducts and ω_{CH4} is the volumetric consumption rate in moles/cm^3/sec. Based on the measurements of CH_4 mole fractions, the Fuel Consumption Rate of IR-excited methane is calculated to be 6 % less than that of regular methane.

Measured CO and CO_2 Distributions

Fig. 10 displays the measured mole fractions of carbon monoxide (CO) and carbon dioxide (CO_2) respectively for regular methane and IR-excited methane. The data show the peak CO emissions of IR-excited methane are about 25% less, compared to regular methane. Due to a faster combustion as indicated in CH_4 measurements, the fuel consumption rate is decreased that resulted in less CO_2 and CO being produced in combustion process, where CO is a precursor of CO_2.

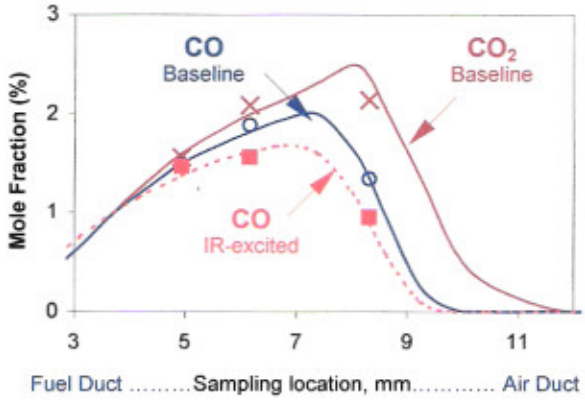

Fig. 10 Measurements of CO and CO_2 mole fractions.

Measured Nitric Oxide (NO) Distributions

The measurements of nitric oxide (NO) emissions are plotted in Fig. 11 for comparisons between IR-excited methane with regular methane. The data show not only a lower peak NO emission with IR-excited methane, but also a smaller area under the curve of NO measurements, indicating less total NO emissions produced during the combustion. Thermal NO formation is always slower than fuel combustion. With a faster combustion, there was less time for NO to form, thus resulting in less NO emissions.

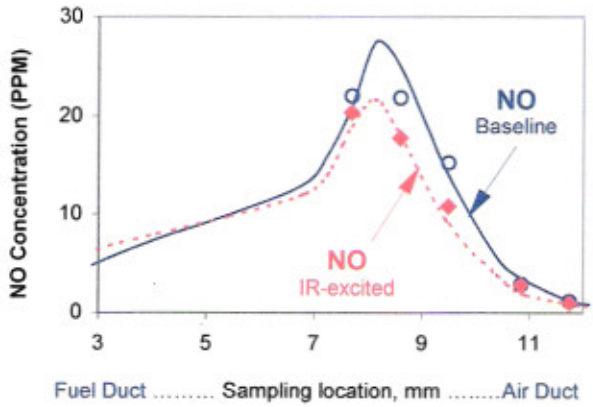

Fig. 11 Measurements of NO emissions.

The ***EIJ***, emission index for species *J* (in this case *J* = NO), is calculated following Takeno and Nishika [18]:

$$EIJ = \frac{\int_0^L M_J \varpi_J\, dx}{\int_0^L M_{CH4} \varpi_{CH4}\, dx}$$

where M_j is the molecular weight of species *J* and ω_J is the volumetric production rate of species *J* in moles/cm^3/s. The EI_{NO}, emission index for NO in combustion of IR-excited methane is computed to be about 15% less than regular methane.

ENGINE-STAND TESTS AT PURDUE

Tests on a GM Quad-4 Gasoline Engine

IR-emitter was installed on a 2000 GM Quad-4 2.4 L gasoline engine at Purdue Engine Labs to demonstrate its effect on the Specific Fuel Consumption (SFC) rates of the engine. The tests were run at variable speeds under a constant load of 20 ft-lb and the data are listed and plotted in Fig. 12, as a function of engine speed RPMs. An average improvement of 6% in fuel consumption over the test speeds range is observed with IR-emitter installed.

Speed RPM	SFC-Baseline	SFC-w/FIR	Improvement
1800	0.8369	0.7839	- 6.76%
2200	0.8381	0.7852	- 6.74%
3000	0.8072	0.7693	- 4.93%

(SFC unit: lb/hp-hr)

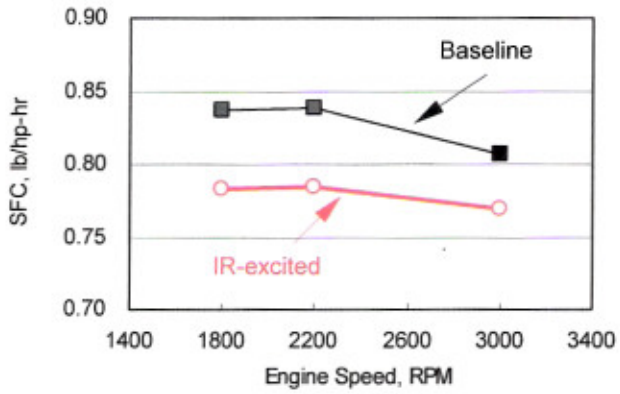

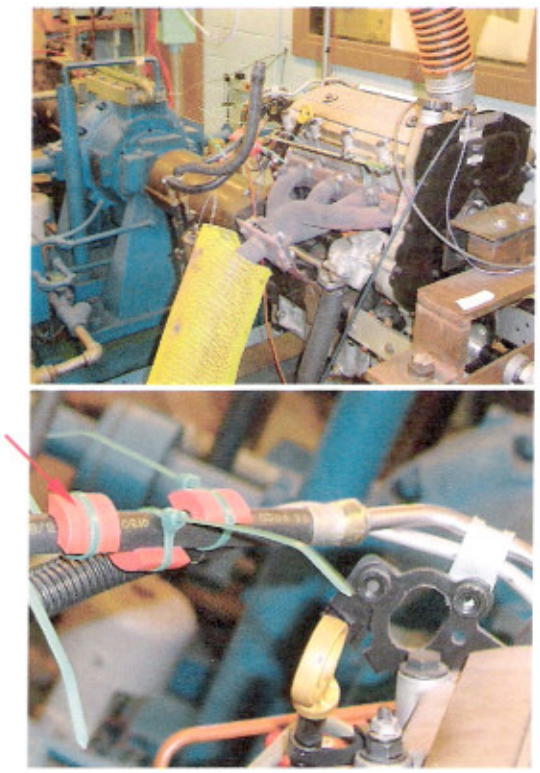

Fig. 12 SFC measurements on a GM Quad-4 engine.

Emissions on a Single-cylinder Engine

IR-emitter was tested at Engine Lab of Purdue University on a PowerTek Single-Cylinder Engine/Dynamometer, as shown in Fig. 13. The engine displacement is 213 cc with a rated maximum power of 5.6 kW. The test was performed at various engine speeds (1000, 1500 and 2000 rpms) under a 40% constant load. Propane fuel was used to verify IR-effect on reducing CO and NOx emissions. The data were automatically collected and are displayed in Table 4, which show an average 14.5 % reduction in CO and 10.2 % reduction in NOx emissions, respectively.

Table 4. CO & NOx Emissions test with propane fuel

	CO (ppm)			NOx (ppm)		
RPM	1500	2000	2500	1500	2000	2500
Baseline	542	1051	1596	254	95	37
R-emitter	468	820	1472	247	79	33
Change %	-13.7	-22.0	- 7.8	- 2.8	- 16.8	- 10.8

Fig. 13 PowerTrek single cylinder dynomometer.

BETA-SITE VHEICLE TESTS

Emissions on a Chinese Iveco Diesel Engine

IR-emitter was tested at Shanghai Vehicle Performance Testing Center (Shanghai, China) on a light-duty pickup shown in Fig. 14, which has a 4-cyl. 2.8 L diesel engine with a rated 87 kW maximum power, made in 1997 by Iveco-China. The tests were performed following standard Chinese testing protocols. The vehicle ran on a dynomometer at variable speeds with a preset 60 N.m load. The results on NOx and smoke emissions are listed in Table 3. It seen that both NOx and smoke emissions are simultaneously reduced, which might seem counter-intuitive, becuase it is generally belived that a tradeoff between NOx and smoke exists. Nevertheless, the simultaneous reduction in both pollutants can be explained by the results from aforementioned methane-air counterflow flame experiments.

Table 3 Test results on Iveco light-duty diesel engine.

(a) NOx Emissions, ppm

Speed, km/h	30	40	50	60	Avg.
Baseline	642	567	505	431	
w/ IR-Emitter	598	530	463	410	
Change	-6.8%	-6.5%	-8.3%	-4.6%	-6.6%

(b) Smoke Emissions, % Opacity

Speed, km/h	30	40	50	60	Avg.
Baseline	16.6	15.8	10.6	6.6	
w/ IR-Emitter	12.4	11.2	7.3	6.0	
Change	-25.3%	-29.1%	-31.1%	-9.1%	-23.7%

Fig. 14 An Iveco diesel pickup tested by the Shanghai Vehicle Performance Testing Center.

Improved Performance of Diesel School Bus

Beta-site tests were also conducted on school buses at a community school district of Greenwood, Indiana. The test bus was a 2004 International CE School Bus, having a modern International VT365 V-8 6.0 L diesel engine with EVRT technology, shown in Fig.15. It ran a regular 60-mile route each school day. The driver carried a fuel card, with which the number of gallons of diesel re-fueled was automatically recorded with the odometer-mileage and data sent directly to fleet supervisor's computer for filing.

Fig. 15 An International School Bus with IR-emitter.

The graph in Fig.16 was generated by using the recorded fueling data. The Baseline fuel economy was computed to be 5.67 miles per gallon (MPG), based on the fueling records over nearly a year from 9/1/04 thru 10/14/05. IR-emitter was installed on 10/14/05 and data were collected for ensuing six months, 10/14/05 – 5/8/06. The average fuel economy with IR-emitter is computed to be 6.23 MPG. Later, IR-emitter was removed on 5/8/06 and the average fuel economy decreased to 5.41 MPG, near its previous baseline. The improvement on fuel economy by using IR-emitter is calculated to be about 12%.

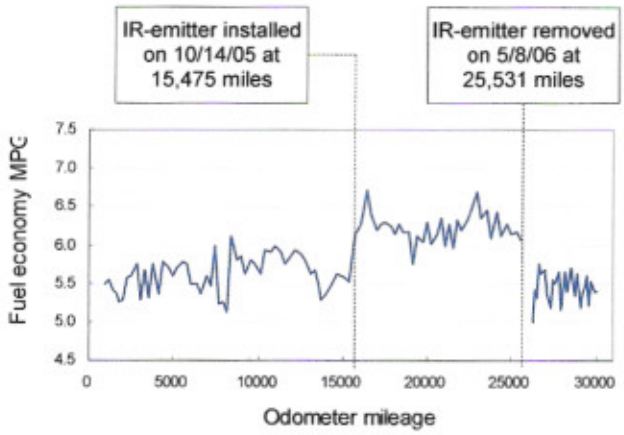

Fig. 16 Refueling records on an International School Bus.

SUMMARY AND CONCLUSIONS

We have developed an innovative technology using 3 – 14 μm wavelength mid-infrared to excite hydrocarbon fuels for increased combustion efficiency in internal combustion engines. IR-emitter can be made from selective transition metal oxides by sintering the mixture of powders and bonding agents at 1300°C. When retrofitted to the exterior of a nonmetal supply fuel line of an engine, the IR-emitter absorbs radiation heat from the engine and emits IR photons in 3 – 14 μm wavelengths. IR photons in this wavelength range can penetrate nonmetal fuel hose and excite the fuel traversing through the fuel line.

The HC molecule in fuel absorbs a number of IR-photons at assorted wavelengths, known as molecular multiphoton process (MMP), causing molecular vibrations. Excited hydrocarbon's constituent electrons can climb up the ladder of vibrational states and reach excited states. IR-excited fuel has lowered activation barrier for reaction with increased combustibility to burn faster in cylinders, allowing more heat released from the fuel in early cycle to do mechanical work and less in later cycle as heat loss to raise exhaust gas temperature (EGT).

In essence, the IR-emitter works as an energy converter that absorbs radiation heat from the engine and emits IR photons. These photons are used to excite hydrocarbons and promote heat release in earlier cycle, allocating more heat to do work and less heat to raise EGT. This results in increased power, lower specific fuel combustion and reduced HC, CO, NOx, and CO_2 emissions.

Based on the preliminary lab investigations and beta-site engine and vehicle tests, conclusions of the present study can be made as follows:

1. IR-excitation causes the counter-flow methane-air to combust faster, resulting in reduced fuel consumption and decreased CO and NO emissions.
2. Hydrocarbons are infrared-active so that IR-excitation will work on all HC-based fuels, including natural gas (methane), propane, gasoline, diesels and bio-diesels.
3. IR-excitation helps reduce Specific Fuel Consumption and all targeted emissions such as HC, CO, NOx, and CO_2 from gasoline or diesel engines.

Though the present study has demonstrated IR-excitation effect is factual in various tests, how it participates in the thermochemical process of combustion remains to be experimentally studied. The IR-excited fuel technology provides a fuel-pretreatment means for increasing combustion efficiency of gasoline and diesel engines. It can be retrofitted on nearly all old or new production engines that are currently in use without changing the engine specifications. Yet, how IR-excited fuel actually improves gasoline and diesel engine performance needs be experimentally examined in details before a conclusion can be made. Future research on optimizing IR-emitting composition is also required.

ACKNOWLEDGMENTS

The authors wish to thank Professor Joseph F. Kmec and his students at Engine Laboratories, Dept. of Mechanical Engineering Technology, Purdue University, for testing IR-device on GM Quad-4 gasoline engine, and Professor Sara E. Leach, Dept. MET, Purdue University, for compositional analysis on IR-emitter. Thanks extended to fleet personnel at the Greenwood Community Schools District and Heritage Transport for voluntarily participating in the beta-site school bus and truck tests. Last, but not least, sincere thank to Mr. Paul D. Davis, Group Transportation Manager, Nestlé U.S.A., for his kind support and valuable leadership in implementing the fleet testing program.

CONTACTS

Albert C. Wey, Inventor of the IR-Excited Fuel technology; B.S. in Electrophysics from Taiwan Chiao-Tung University (1977), Ph.D. (1985) degrees in Electrical Engineering from the State University of New York at Stony Brook; MBA degree from the University of Chicago (1994); e-mail: wey.albert@yahoo.com Phone: (630) 632-1415.

Rodney G. Handy, Associate Professor, Department of Mechanical Engineering Technology, Purdue University, e-mail: rhandy@purdue.edu

Yuan Zheng, Research Assistant Professor, Maurice J. Zucrow Laboratories, School of Mechanical Engineering, Purdue University, e-mail: zhengy@ecn.purdue.edu

REFERENCES

1. Wey A, "Effect of Infrared-Irradiated Fuels on Smoke Reduction of A Diesel Engine – An Initial Study", Proceedings of AFS Fall 2003 Topical Conference, 9/30 – 10/2. Ann Arbor, MI.
2. Smith M, "Organic Chemistry", Harper Collins Publisher, New York (1993), p. 413.
3. Turro N J, "Modern Molecular Photochemistry", Benjamin-Cummins, Menlo Park, 1978.
4. Chiu T. H., "The Principle and Application of Far-Infrared Heating", 1995, Wen-Seng Publisher, Taiwan, p. 31 – 45.
5. Wey A, "Infrared-Irradiated Fuels for Increased Fuel Conversion Efficiency", Proceedings of AFS Fall 2005 Topical Conference, 9/19 – 22. Ann Arbor, MI.
6. Lim J., Gore J., and Viskanta R., "A Study of the Effects of Air Preheat on the Structure of Methane/Air Counterflow Diffusion Flames", Combustion and Flame 121, p. 262 – 274 (2000)
7. Lutz A. E., Kee R. J., Grear J. F., and Ruply F. M., Sandia Report SAND96-8243 (1996).
8. Kee R. J., Miller J. A., Evans J. H., and Dixon-Lewis G., 22nd Symposium (International) on Combustion, p. 1479 – 1495 (1988).
9. Bowman C. T., Hanson R. K., Davidson D. F., Gardiner Jr. W. C., Lissianski V., Smith G. P., Golden D. M., Frenklach M., and Goldenberg M., http://www.me.berkeley.edu/gri_mech. GRI-Mech 2.11 (1996)
10. Chemical Physics Handbook, "Infrared Correlation Chart," p. 9-87 – 9-89 (2004)
11. Evans M. G. and Polanyi M., Trans. Faraday Soc., 35, P. 178 (1939)
12. Karny Z. and Zare R. N., J. Chem. Phys., 68, 3360 (1978)
13. Reiser C, MIT Ph.D. Thesis, "Mechanism of Multiple Infrared Photon Absorption and Dissociation" (1980).
14. Mukamel S. "Reduced Equations of Motion for Collisionless Molecular Multiphoton Process", Photoselective Chemistry, Adv. Chem. Phys., vol. 47 (1981) p. 509.
15. Weitz E and Flynn G, "Vibrational Energy Flow in the Ground Electronic States of Polyatomic Molecules", Photoselective Chemistry, Adv. Chem. Phys., vol. 47 (1981) p. 185.
16. Atkins P.W., "Quanta", Oxford University Press, New York, 1991, P. 101
17. Puri I. K., Seshadri K., Smooke M. D., and Keys D. E., Combustion Science Technology, vol. 56, p. 1 – 12 (1987).
18. Takeno T., and Nishioka M., Combustion Flame 92, p. 465 – 468 (1993).